Icarus 210 (2010) 92–101

Contents lists available at ScienceDirect

Icarus

journal homepage: www.elsevier.com/locate/icarus

Pedestal crater heights on Mars: A proxy for the thicknesses of past, ice-rich, Amazonian deposits

Seth J. Kadish [a,*], James W. Head [a,1], Nadine G. Barlow [b,2]

[a] Brown University, Department of Geological Sciences, 324 Brook St., Box 1846, Providence, RI 02912, USA
[b] Northern Arizona University, Department of Physics and Astronomy, NAU Box 6010, Flagstaff, AZ 86011, USA

ARTICLE INFO

Article history:
Received 18 January 2010
Revised 4 June 2010
Accepted 17 June 2010
Available online 30 June 2010

Keywords:
Mars
Cratering
Impact processes
Ices

ABSTRACT

Mid-latitude pedestal craters on Mars offer crucial insights into the timing and extent of widespread ice-rich deposits during the Amazonian period. Our previous comprehensive analysis of pedestal craters strongly supports a climate-related formation mechanism, whereby pedestals result from impacts into ice-rich material at mid latitudes during periods of higher obliquity. The ice from this target deposit later sublimates due to obliquity changes, but is preserved beneath the protective cover of the armored pedestal. As such, the heights of pedestals act as a proxy for the thicknesses of the paleodeposits. In this analysis, our measurement of 2300 pedestal heights shows that although pedestals can reach up to ~260 m in height, ~82% are shorter than 60 m and only ~2% are taller than 100 m. Mean pedestal heights are 48.0 m in the northern mid latitudes and 40.4 m in the southern mid latitudes, with the tallest pedestals located in Utopia Planitia, Acidalia Planitia and Malea Planum. We use these data in conjunction with prior climate model results to identify both regional and global trends regarding ice accumulation during obliquity excursions. Our data provide evidence for multiple episodes of emplacement and removal of the mid-latitude ice-rich deposit based on stratigraphic relationships between pedestal craters and the close proximity of pedestals with significantly different heights.

1. Introduction

We have recently presented a range of evidence for a sublimation-driven formation mechanism for pedestal craters on Mars (Kadish et al., 2008, 2009). First recognized in Mariner 9 data (McCauley, 1973), pedestal craters are an impact crater morphology on Mars characterized by a crater perched near the center of a plateau, surrounded by an often-circular, outward-facing scarp (Arvidson et al., 1976; Barlow et al., 2000). We have mapped 2300 pedestal craters from 60°N to 65°S to establish the latitude-dependent distribution and have physically characterized the pedestal craters' attributes (Kadish et al., 2009). We also have identified pedestal craters in Utopia Planitia and Malea Planum that have marginal pits, providing evidence for the sublimation of volatiles from the scarps of the pedestals (Kadish et al., 2008). This work further supports a model that calls on impact into ice-rich targets to produce pedestal craters during periods of higher obliquity, when mid to high latitudes were covered by thick deposits of snow and ice (Fig. 1). During return to lower obliquity (e.g. Head et al., 2003; Levrard et al., 2004), the regional volatile-rich unit sublimated, lowering the elevation of the surrounding terrain and removing its exposed snow and ice. Beneath the armored cover of the pedestals, however, the ice-rich deposit is preserved (Fig. 2).

It is important to note that the armoring and the ejecta are not the same feature. The armoring is the result of sintering and induration of the region proximal to the impact event. The exact mechanism by which the surface becomes armored remains debated, and several processes have been proposed. These include a coarse ejecta covering or lag deposit (Arvidson et al., 1976), increased ejecta mobilization caused by volatile-rich target substrates (e.g. Osinski, 2006), impact melt distribution that produces a glassy veneer (Schultz and Mustard, 2004), an atmospheric blast followed by a high temperature thermal pulse (Wrobel et al., 2006), and a turbulent, dust-laden, density-driven flow (Boyce et al., 2008). Although we have identified instances of single-layer ejecta distributed on pedestal surfaces, consistent with past observations (Mutch and Woronow, 1980; Barlow, 2004, 2006), the ejecta is always much more limited than the extent of the armoring that produces the pedestal surface. As such, the primary constraint that our empirical observations has on the armoring mechanism is that it must be capable of affecting an anomalously large lateral area. This

* Corresponding author. Fax: +1 401 863 3978.
E-mail addresses: Seth_Kadish@Brown.edu (S.J. Kadish), James_Head@Brown.edu (J.W. Head), Nadine.Barlow@NAU.edu (N.G. Barlow).
[1] Fax: +1 401 863 3978.
[2] Fax: +1 928 523 1371.

0019-1035/$ - see front matter © 2010 Elsevier Inc. All rights reserved.
doi:10.1016/j.icarus.2010.06.021

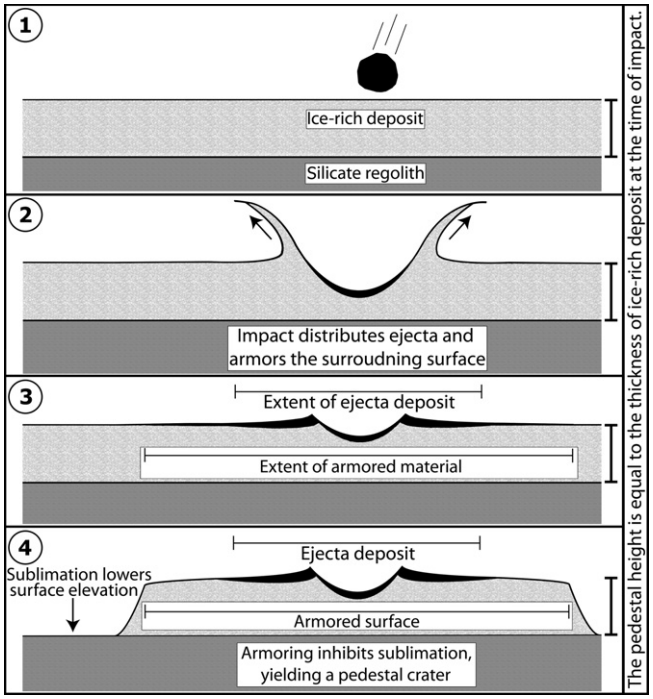

Fig. 1. A schematic diagram of the primary steps in the sublimation model of pedestal crater formation (altered from Kadish et al. (2009)), highlighting that the thickness of the target material, which is an ice-rich deposit, is the eventual height of the pedestal. The steps are: (1) Impact into an ice-rich deposit that has accumulated at mid latitudes during a period of higher obliquity over the martian silicate regolith. (2) The impact distributes ejecta and triggers an armoring process. (3) This results in a radially-symmetric armored surface around the crater rim that exceeds the extent of the ejecta deposit. (4) During return to lower obliquity, volatiles sublimate from the unarmored intercrater terrain, lowering the elevation of the surrounding terrain. Armoring inhibits sublimation from beneath the pedestal surface, preserving the ice-rich deposit. This results in a typical pedestal crater that is as tall as the initial thickness of the target deposit.

suggests that the armoring mechanism is unlikely to be ballistic in nature. For a discussion of the proposed armoring mechanisms and of the pedestal extent as measured by the pedestal to crater radius ratio, see Sections 3.2, 4.1, and 4.6 of Kadish et al. (2009).

In this sublimation model, the heights of pedestal craters are a proxy for the thickness of the paleodeposit and provide information as to how it may have varied regionally. These data can be used to establish where snow and ice preferentially accumulated during periods of higher obliquity. Here, we provide results on the measurements of mid-latitude pedestal heights, and discuss the implications for the timing and extent of a past latitude-dependent, ice-rich deposit.

2. Methodology

Pedestal height measurements in this study used gridded Mars Orbiter Laser Altimeter (MOLA) data (463 m/pix). Pedestal surfaces are not always level; their slopes are influenced by the topography of their surroundings (Fig. 3). As such, it is not valid to calculate a pedestal height as the difference between the highest elevation of the pedestal and the lowest elevation of the immediately adjacent terrain. To account for this, we made four measurements of each pedestal's elevation, one in each quadrant (NW, NE, SW, and SE), halfway between the pedestal margin and the crater rim. Most pedestal surfaces are smooth, with no remaining topographic or morphologic evidence of the ejecta deposit. As previously mentioned, in cases where the ejecta is preserved, it never covers the entirety of the pedestal surface, and is usually much smaller in its radial extent. In these cases, we took precautions to avoid taking elevation data on the ejecta, ensuring that we were only measuring the elevation of the pedestal surface and not the combined elevation of the pedestal and the ejecta. We then made four measurements of the elevation of the surrounding terrain along the same radial lines extending from the crater center. These were taken within 2 km of the pedestal margin, avoiding topographic aberrations like pits or mounds that would provide spurious results. The average of the four elevations of the surrounding terrain was then subtracted from the average of the four pedestal elevations to get the pedestal height.

This method provides reasonable averages for the heights of the pedestal craters, and works to eliminate the influence of local slopes and uneven terrain. It is possible that the current elevation of the intercrater terrain in some regions is not the same as it was prior to emplacement of the latitude-dependent deposit due to local mantling and/or erosion subsequent to the pedestal crater formation. Although we cannot account for these potential changes to the elevations of the surrounding surfaces, they are likely negligible compared to the heights of the pedestals and should not affect our results on a global scale.

3. Global distribution and trends of pedestal heights

Pedestal heights (Figs. 3 and 4) have important implications for the surface conditions that existed at the time of impact. Previous researchers (e.g. Bleacher et al., 2003; Thomson and Schultz, 2007; Tanaka et al., 2008) have noted that the heights of pedestal craters offer information concerning the elevation of the paleosurface; pedestal craters represent the remnants of a paleodeposit that has since been removed, leaving the craters perched above the surrounding terrain. Our interpretation is that these paleodeposits were emplaced directly on the martian regolith, persisted for some duration of time and were then removed. Given this interpretation, the heights of pedestal craters can act as a proxy for the thicknesses of these paleodeposits. Impacts that occurred into the paleodeposit during its accumulation or removal would produce pedestals that are shorter than the maximum thickness of the deposit. Consequently, some pedestal heights may provide minima for the thicknesses of the regional paleodeposits rather than the full thicknesses.

The use of pedestal heights as a proxy for paleodeposit thickness is valid regardless of which armoring mechanism is eventually

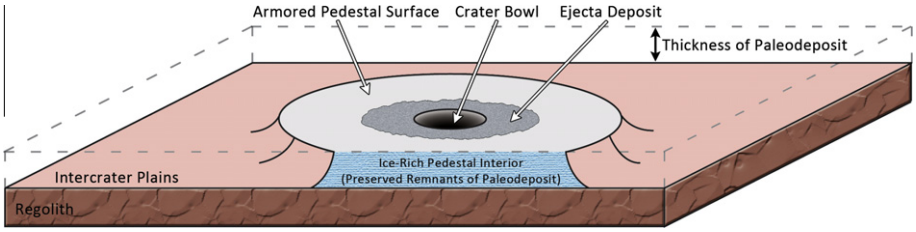

Fig. 2. A perspective view of a pedestal crater. This illustration highlights that: (1) Pedestal craters are elevated above the intercrater plains, with the pedestal height equivalent to the thickness of a past ice-rich paleodeposit. (2) The pedestal interior preserves the paleodeposit under its armored surface, and thus maintains ice-rich material. (3) The ejecta deposit resulting from the impact is much smaller in radial extent than the armored pedestal surface.

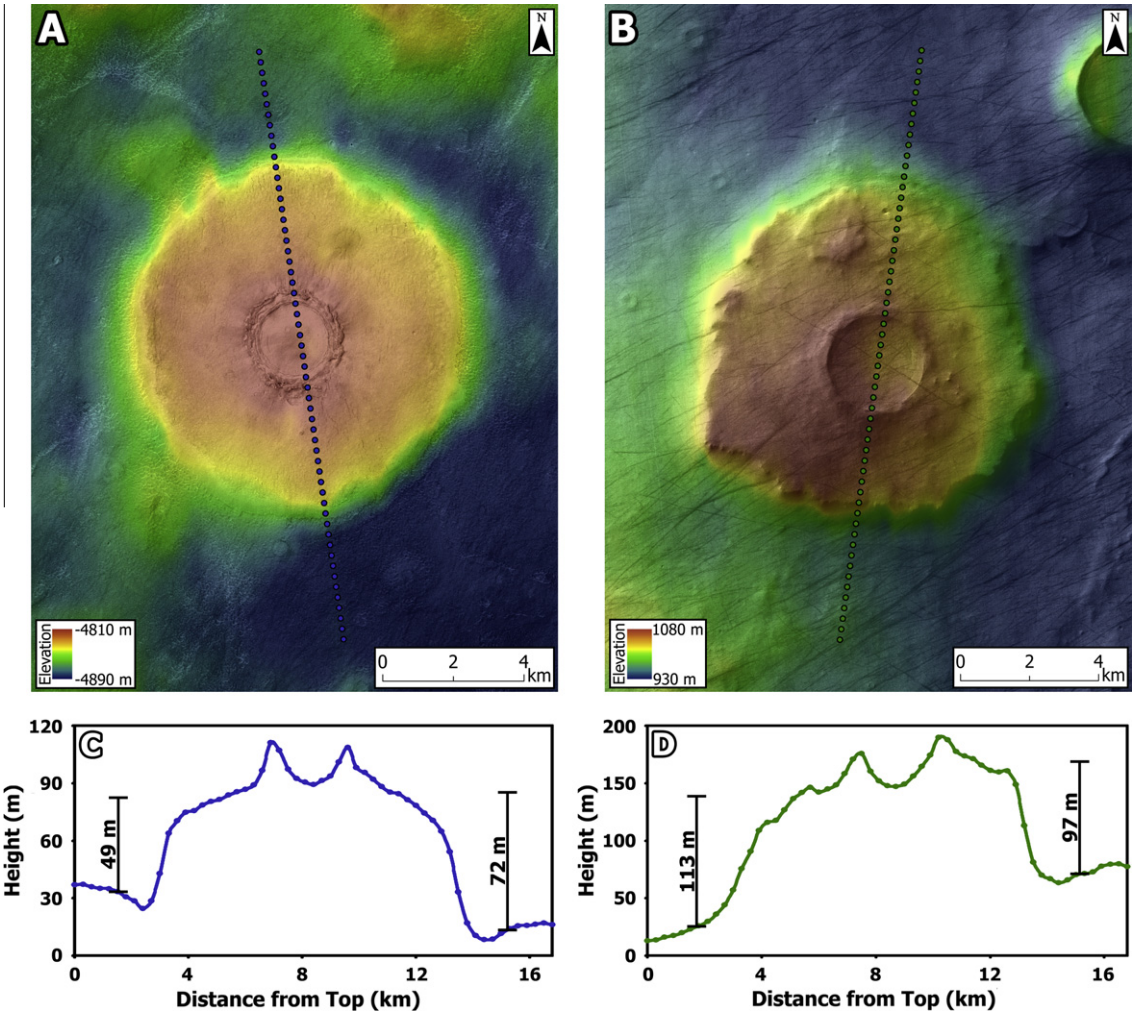

Fig. 3. Examples of pedestal craters shown in CTX images with MOLA topography and corresponding profiles from MOLA shot data. (A) A 2.1-km-diameter crater located in western Utopia Planitia at 48.1°N, 101.3°E (P18_008214_2288). (B) A 2.8-km-diameter crater located west of Malea Planum at 57.2°S, 36.0°E (P15_007004_1222). Note the remnants of a smaller pedestal crater, 0.9 km in diameter, completely superposed on the northern end of the larger pedestal. (C) A profile of the pedestal crater in (A), showing the individual MOLA points (VE = 67x). The surrounding topography is uneven, resulting in heights of 49 m and 72 m on the northern and southern sides of the pedestal respectively. The calculated height of the pedestal is 62 m. (D) A profile of the pedestal crater in (B), showing the MOLA shot data (VE = 40x). The local topography slopes downhill from SW to NE. This slope produces greater pedestal heights on the downhill (northern) side, as shown by the measurements of 113 m and 97 m on the northern and southern sides respectively. The calculated height of the pedestal is 107 m.

proven to be correct, and is consistent with both the eolian deflation model and the climate-related sublimation model for pedestal crater formation. Historically, pedestal craters were thought to form by armoring of a dry, fine-grained target material during the impact event, followed by eolian deflation of the intercrater terrain. This preferential erosion of the non-armored material would yield the perched pedestals surrounded by marginal scarps (e.g. McCauley, 1973; Schultz and Lutz, 1988). However, as previously mentioned, we have provided substantial evidence supporting a formation mechanism involving sublimation of an ice-rich paleodeposit (Kadish et al., 2008, 2009).

Support for the sublimation model includes, but is not limited to, the following: (1) The latitude-dependent distribution of pedestal craters (Fig. 4), with the majority found poleward of 45° (Mouginis-Mark, 1979; Kadish et al., 2008, 2009). The distribution also mimics that of several other surface morphologies that are indicative of a mid-latitude ice-rich substrate, and coincides with the regional and latitudinal extent of where martian climate models predict snow/ice accumulates during periods of higher obliquity (e.g. Richardson and Wilson, 2002; Mischna et al., 2003; Madeleine et al., 2009). This latitude-dependent distribution is at odds with the eolian deflation model, which allows pedestals to form in any region with fine-grained material on Mars. (2) The paucity of pedestal craters larger than 5 km in diameter. The deflation model does not predict any size limitation for pedestal crater formation, but under the sublimation model, large impacts would likely overwhelm an ice-rich unit, melting and/or vaporizing its volatiles upon impact (Barlow et al., 2001). Under the sublimation model, the small size of most pedestal craters may also explain why they rarely have ejecta deposits. Impacts into ice-rich material would distribute the dust/ice mixture on top of the armored surface. When the obliquity lowers and the intercrater terrain sublimates, yielding the pedestal relief, the ejecta would also sublimate and any remaining fines would be prone to deflation. Only in cases where there was a particularly high dust to ice ratio, or the impact excavated and distributed the underlying regolith, would there be enough material to maintain an ejecta deposit on the pedestal surface. (3) Physical measurements of the pedestal craters' attributes (Kadish et al., 2009), as discussed in Section 4. Most importantly, pedestals are extremely circular, which is an expected result from the sublimation model. Eolian deflation of the surrounding terrain would produce elongated pedestals due to predominant wind

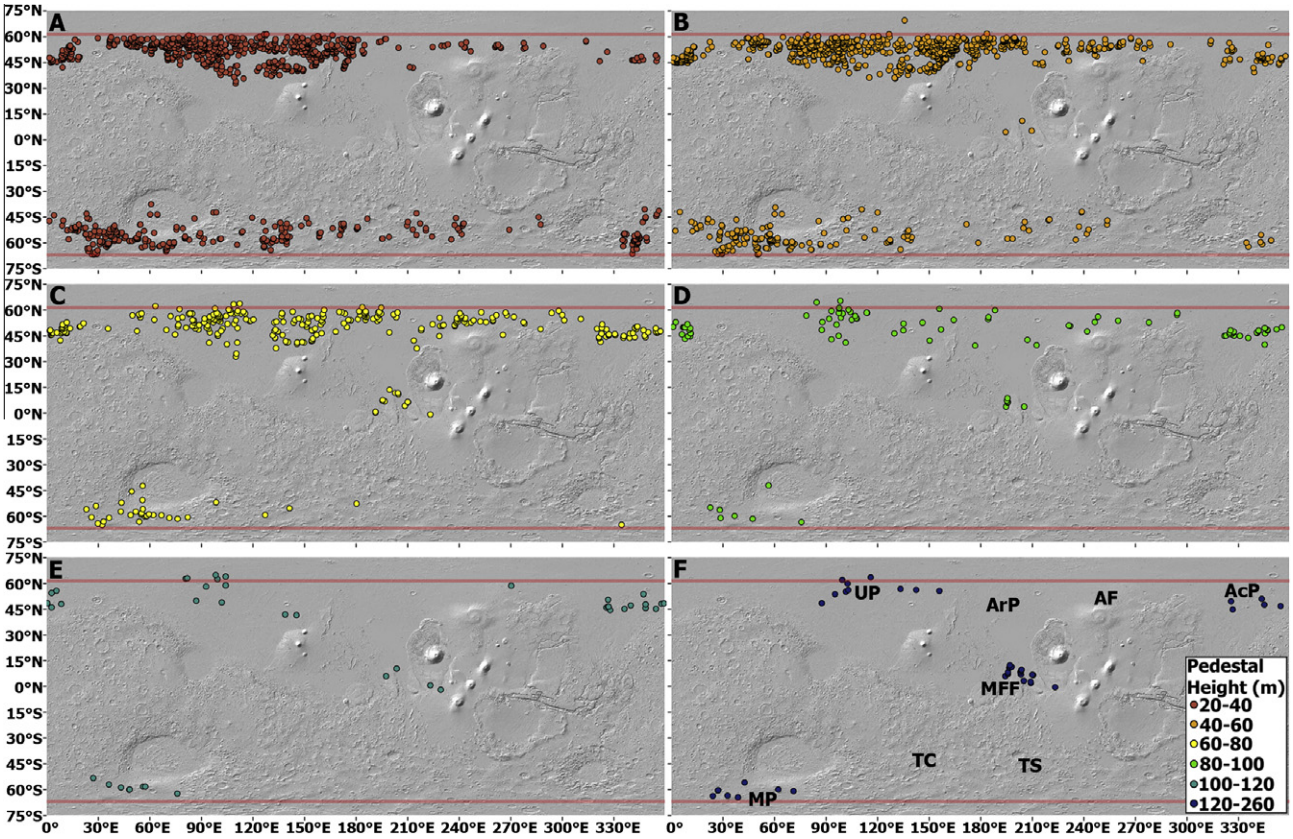

Fig. 4. The geographic distribution of pedestal heights. Pedestal craters were primarily identified through a survey of all THEMIS IR images with center coordinates equatorward of 60°N and 65°S (Kadish et al., 2009). As such, pedestal craters poleward of these latitudes were generally not analyzed in this study – lines on the maps indicate the boundaries of the study region. The populations have been divided into six groups to show where populations of specific heights are concentrated: (A) 20–40 m, (B) 40–60 m, (C) 60–80 m, (D) 80–100 m, (E) 100–120 m, and (F) 120–260 m. Regions discussed in this paper are labeled on map (F), with the following abbreviations: AcP = Acidalia Planitia, AF = Alba Fossae region, ArP = Arcadia Planitia, MFF = Medusae Fossae Formation, MP = Malea Planum, TC = Terra Cimmeria, TS = Terra Sirenum, and UP = Utopia Planitia.

directions. (4) Pits in the scarps of some pedestal craters, as discussed in Section 5.3, indicating a loss of material from the pedestal itself (Kadish et al., 2008). These pits are morphologically similar to scallops and other sublimation depressions, and they never excavate below the elevation of the surrounding terrain. This suggests that pedestals are composed of ice-rich material overlying a dry/desiccated regolith.

Given this evidence for a sublimation-driven formation mechanism and the notion that pedestal heights are reasonable proxies for the thicknesses of the paleodeposits, we can use our measurements in conjunction with other pedestal crater attributes to constrain the distribution, volume, and timing of ice accumulation at mid latitudes during periods of higher obliquity. The geographic distribution of pedestal heights on Mars reveals four important trends (Figs. 4 and 5 and Table 1): (1) Pedestals tend to be <60 m in height (Fig. 5A). Although we measured pedestals as tall as 256 m, only 43 of 2300 (~2%) were >100 m, while 1885 of 2300 (~82%) were <60 m. Pedestals <20 m in height were not analyzed in this study due to the uncertainty in distinguishing them from regular craters with thick ejecta deposits. (2) Although pedestals are, on average, slightly taller in the northern hemisphere (48.0 m) than the southern hemisphere (40.4 m), the average height of mid-latitude pedestals does not show any statistically significant variation as a function of latitude (Fig. 5B). As we will discuss later, this result is most likely due to the high population density of short pedestals (20–50 m) at both mid and high latitudes, masking the tendency of the less populous tall pedestals (>80 m) to form at higher latitudes. The small equatorial population, located exclusively in the Medusae Fossae Formation (MFF), is composed of much taller pedestals; the mean height is 114.4 m compared to 47.7 m at mid latitudes in both hemispheres. It is important to note that MFF pedestal craters are morphologically distinct from those at mid latitudes, and may result from an entirely different formation mechanism (Kadish et al., 2009). (3) Within each hemisphere, there are variations in pedestal height as a function of longitude (Fig. 5C and D). The mapped distribution of pedestals >80 m in height (Fig. 4D–F) shows that the tallest mid-latitude pedestals are concentrated in Utopia Planitia and Acidalia Planitia in the northern hemisphere and Malea Planum in the southern hemisphere. As a result, the average pedestal height in Acidalia Planitia and Malea Planum is slightly greater than the average in the rest of their respective hemispheres. Utopia Planitia, however, also contains the highest concentration of shorter pedestals, resulting in a lower average height for the region compared to the rest of the northern hemisphere. (4) Pedestals in close proximity to each other can have significantly different heights; we see examples of pedestal craters less than 20 km apart that have a height difference of more than 80 m. This is especially common in Utopia Planitia. As will be discussed later, this heterogeneity in regional pedestal heights suggests that pedestals are likely forming from multiple distinct episodes of obliquity excursions.

4. Relationship between heights and other pedestal attributes

In addition to pedestal heights, we have measured three other key pedestal crater attributes (Kadish et al., 2009). These include the diameter of the crater bowl, pedestal to crater radius ratio (*P*/

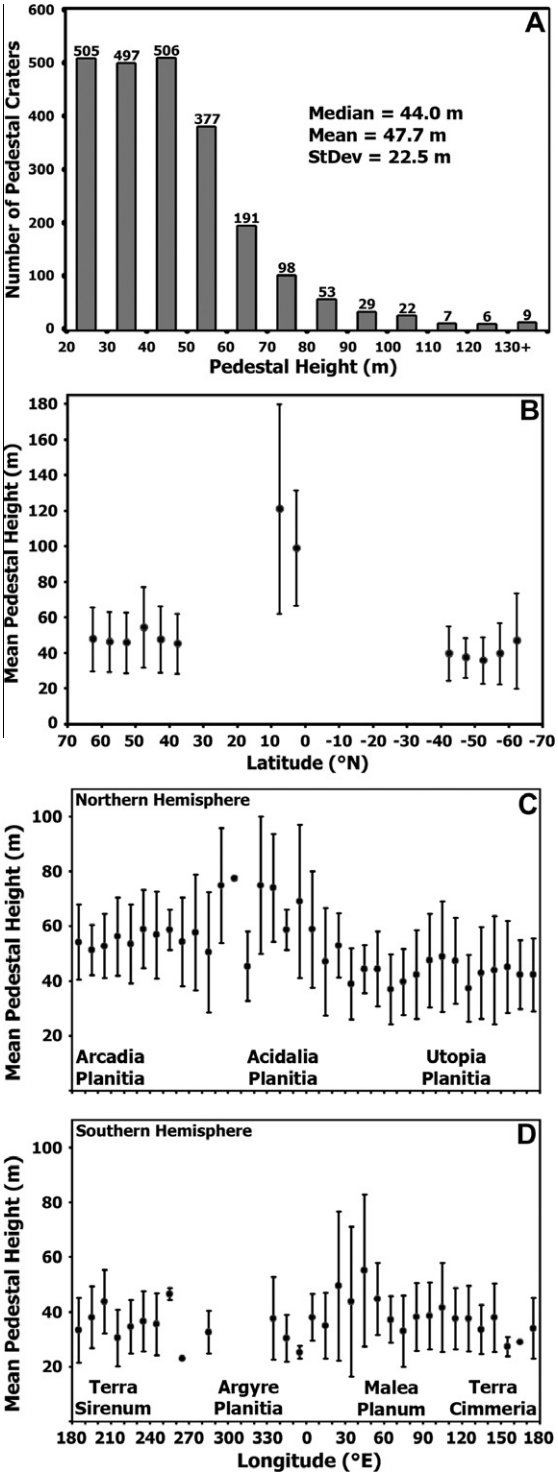

Fig. 5. The quantitative results of this study in the form of: (A) A histogram of the pedestal height distribution for all 2300 pedestals measured. The median, mean and standard deviation of the pedestal heights for the population are shown. (B) Mean pedestal heights as a function of latitude. Pedestals are slightly taller in the northern than in the southern hemisphere, but neither shows significant variations as a function of latitude. Equatorial pedestals, located in the MFF, have much greater heights than those at mid latitudes. Error bars in B–D are ±1 standard deviation. (C) Mean mid-latitude pedestal heights in the northern hemisphere as a function of longitude. (D) Mean mid-latitude pedestal heights in the southern hemisphere as a function of longitude. Because equatorial pedestal craters are confined to the MFF, we have not shown their variations as a function of longitude.

C ratio – similar to "ejecta mobility ratio" for layered ejecta morphologies) (e.g. Mouginis-Mark, 1979; Barlow, 2004), and pedestal

Table 1
Statistics for pedestal heights on Mars (meters).

	Median	Mean	Standard deviation
All mid latitude	44.0	47.7	22.5
Northern mid latitude	45.0	48.0	18.8
Southern mid latitude	35.0	20.4	19.2
Equatorial (MFF)	95.0	114.4	53.0

circularity value (equivalent to "lobateness" for layered ejecta morphologies) (e.g. Barlow, 1994), where:

$$P/C \text{ ratio} = (\text{farthest extent of pedestal})/(\text{crater radius}) \quad (1)$$

$$\text{Pedestal circularity} = (\text{pedestal perimeter})/(4\pi(\text{pedestal area}))^{1/2} \quad (2)$$

These three attributes are established by the impact and armoring processes. The *P*/*C* ratio is dependent on the size of the crater and the radial extent of the armoring, while the pedestal circularity is solely dependent on the radial symmetry of the armoring. If the pedestal height is determined exclusively by the thickness of the ice-rich target material, then the height should be independent of both the impact and armoring process, and therefore be independent of the *P*/*C* ratio and the pedestal circularity.

To test these potential relationships between pedestal crater traits, we have plotted pedestal heights against each of the other three attributes (Fig. 6). The correlation coefficients of these graphs are all positive values less than 0.09; we observe no statistically significant relationship between the pedestal height and the crater size, pedestal size, or pedestal shape. While this does not guarantee that pedestal height is solely the result of the thickness of the target deposit, it greatly reduces the possibility that our data have any bias from the cratering and/or armoring processes. It should be noted that these results do not favor one pedestal crater formation mechanism over another. Both the eolian deflation model and the sublimation model predict that the pedestal height is determined by the thickness of the target layer and not the impact process. We thus present these data not to further our support for the sublimation model, but to provide additional support for our fundamental assertion that pedestal heights can be used to approximate the thicknesses of regional paleodeposits.

5. Discussion

5.1. Geographic extents of the ice-rich deposits

We have shown that the heights and locations of pedestal craters can provide insight into both the geographic extents and thicknesses of the mid-latitude ice-rich deposits from which the pedestals formed. Given the sublimation-driven formation mechanism, we would expect that the highest concentrations of pedestal craters delineate regions where the ice-rich deposits persisted for the longest periods of time, and the tallest pedestal craters highlight where the deposits reached the greatest thicknesses.

In our study region, there are approximately 3.6 times more pedestal craters in the northern hemisphere than in the southern hemisphere. If the regional concentration of pedestal craters is viewed as an estimate of the duration of snow/ice cover, then the geographic distribution (Fig. 4) suggests that the ice-rich deposits persisted for longer in the northern mid latitudes. Within the northern hemisphere, the ice-rich deposits were widespread and persisted for the longest in Utopia Planitia. Acidalia and Arcadia Planitia were likely also covered by long-standing ice-rich deposits. The deposits were present for much shorter durations of time in the Alba Fossae region. In the southern hemisphere, the deposits

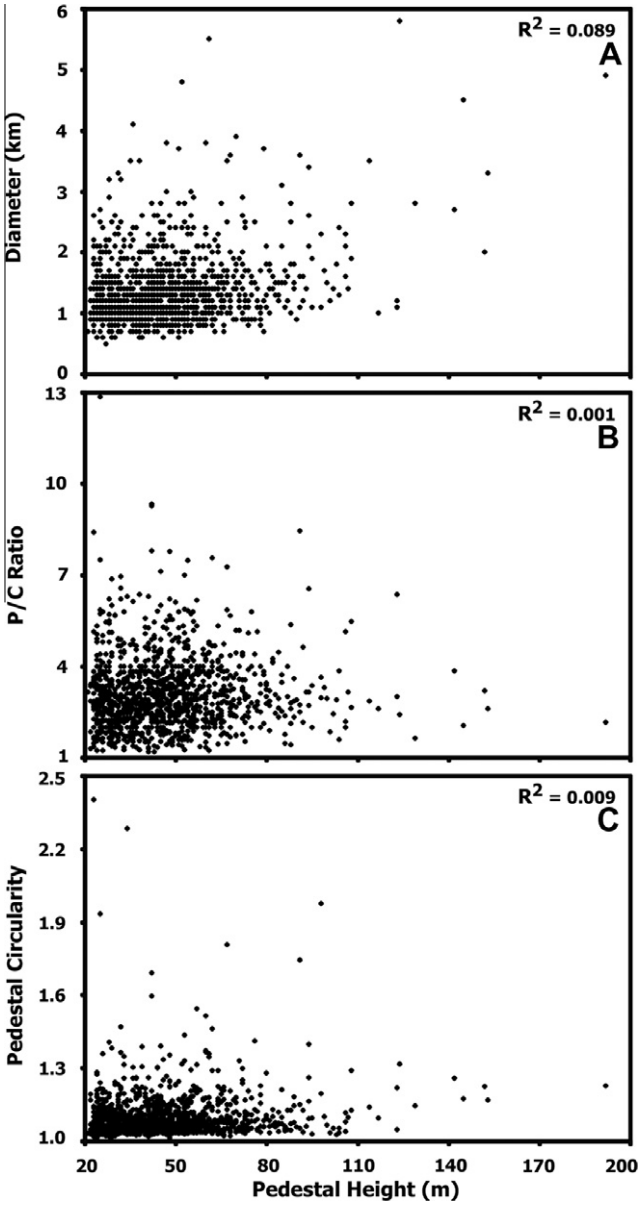

Fig. 6. Plots of pedestal height versus: (A) Crater diameter, (B) *P*/*C* ratio, and (C) pedestal circularity. These attributes, measured and described by Kadish et al. (2009), are the result of the impact/armoring process. The correlation coefficients for linear fits to the data are shown in the top right corner of each plot. These extremely low values confirm that there is no statistically significant correlation between the pedestal heights and the impact size or extent of the armoring.

remained for the longest periods of time in Malea Planum, which has roughly the same population density as Arcadia Planitia. The deposits were emplaced for much shorter durations near Terra Cimmeria and Terra Sirenum.

The distribution of pedestal heights, however, suggests that the emplacement duration and maximum thickness are not directly correlated. The locations of mid-latitude pedestals taller than 80 m (Fig. 4D–F) reveal that the thickest deposits accumulated in Utopia Planitia, Acidalia Planitia, and Malea Planum. The maximum pedestal heights in these regions are 131 m, 152 m, and 192 m, respectively. These data show that, although the ice-rich material may have been present the longest in Utopia Planitia, the thickest accumulations may have been briefly present in Malea Planum, and to a lesser extent, Acidalia Planitia. In addition, Arcadia Planitia, which has a higher concentration of pedestal craters than Acidalia, has no pedestals taller than 100 m, suggesting a long-standing deposit formed by steady but low accumulation rates. The Alba Fossae region, which has a low pedestal crater population density, also lacks pedestals taller than 100 m, but has more pedestals that are 50–80 m tall than 20–50 m tall. This implies a short-lived ice-rich deposit that accumulated rapidly, remained at maximum thickness for the majority of its lifetime, and then quickly sublimated.

The absence of a latitude-dependent change in average pedestal height, as mentioned in Section 3, may have important implications for the nature of the ice-rich paleodeposits. This trend, in conjunction with noted variations in longitudinal thickness, may suggest that the deposits that produced the pedestal crater population are not the result of simple migration of volatiles from the poles to the mid latitudes during periods of higher obliquity (Head et al., 2003), which might produce taller pedestals at higher latitudes. Rather, these deposits could be regional in nature, with peak accumulation zones occurring due to mesoscale changes in topography and wind, resulting in deposits centered across a variety of latitudes. We find this to be unlikely, however, given the dominant latitude-dependence of climatic factors. Instead, we interpret this trend to be a statistical result of averaging the heights of a large population of short pedestals (20–50 m) with a small population of tall pedestals (>80 m); short pedestals outnumber tall pedestals by a count of 1508 to 126, or a ratio of ~12:1. A qualitative assessment of the geographic distribution suggests that short pedestals have a high population density at all latitudes where pedestal craters can form, excluding the MFF, while tall pedestals tend to be restricted to the higher latitudes within our study boundaries (Fig. 4). This distribution is consistent with a climate scenario where the thickest paleodeposits accumulated and were maintained for the longest periods of time poleward of ~50° latitude in both hemispheres, while thinner, more transient deposits accumulated between 35° and 50° latitude (e.g. Head et al., 2003).

Climate modeling research can be used in tandem with our empirical data to strengthen our interpretations regarding mid-latitude accumulations of ice-rich material. Recent climate modeling research (Madeleine et al., 2009) using an equatorial source of ice on the flanks of the Tharsis volcanoes (Forget et al., 2006) has shown that glaciations can readily occur in the northern mid latitudes. The model produces ice accumulation rates of ~10 mm/yr given a moderate obliquity (25–35°) (Madeleine et al., 2009). This result is supported by previous climate modeling research, which has shown that that during periods of moderate obliquity (35°), the zone of water–ice stability extends to the mid latitudes, and at higher obliquities (45°), water–ice is stable at tropical latitudes (Richardson and Wilson, 2002; Mischna et al., 2003). We must be cautious when comparing our results to any given modeling output due to the high number of variables; the parameter space used by Madeleine et al. (2009) includes the orbital eccentricity, obliquity, areocentric longitude of the Sun at perihelion, dust optical depth, and location of the surface water–ice reservoir. Our pedestal crater distribution does, however, closely match the regions in the northern mid latitudes predicted to have highest accumulation rates under dusty conditions at 35° obliquity. This output used an eccentricity of 0.1 and an aphelion during the northern summer, and yields net ice accumulation of 10–16 mm/yr in western Utopia Planitia and rates of 8–12 mm/yr in Acidalia and Arcadia Planitia (see Fig. 7 in Madeleine et al. (2009)). Continued modeling work will further constrain the orbital and atmospheric conditions necessary to form the deposits that produced the pedestal crater population.

5.2. Timing and recurrence of the ice-rich deposits

The geographic distribution of the pedestal craters and the proximity relationships between pedestals of different heights

constrain the timing and recurrence of the mid-latitude ice-rich deposits. As discussed, we commonly observe pedestals in close proximity (10s of km) that are up to 80 m different in height. In addition to these examples, we have identified more than 30 instances of pedestal craters that are partially draped over the scarps or completely superposed on the surfaces of other pedestal craters (Figs. 3B and 7–9; also see Fig. 16 in Kadish et al. (2009)). While pedestals in close proximity that have extremely different heights could potentially form from the same deposit at different times – one during the early stage of accumulation or late stage of sublimation and another during maximum thickness of the deposit – it is much more difficult to explain draped pedestals, which show the topographic influence of the underlying pedestal scarp. These cases of draped pedestals require one pedestal to form completely, followed by an impact into a subsequent deposit that contours to the topography of the underlying pedestal (Figs. 8 and 9). In the context of this evidence for recurring depositions of mid-latitude ice-rich deposits, it is highly likely that the pedestal crater population measured in this study formed from multiple episodes of accumulation and sublimation.

The recurrence of these mid-latitude ice-rich deposits is supported by the known variations in martian obliquity over the past 20 Myr (Laskar et al., 2004). The obliquity of Mars over the last 5 Myr has oscillated between 15° and 35°, and during the previous 15 Myr, it oscillated between 25° and 45°. Given the modeled exchange of volatiles between the poles, mid latitudes, and equatorial regions at these obliquities (e.g. Forget et al., 2006; Madeleine et al., 2009) and the high frequency of the recent obliquity variations (e.g. Laskar et al., 2004; Levrard et al., 2004), it is expected that ice-rich material has been repeatedly emplaced and removed at mid latitudes throughout the Late Amazonian. Assuming an accumulation rate of 10 mm/yr (Madeleine et al., 2009), it would take only 5 kyr to form a 50 m deposit, which is thick enough to produce an average pedestal. Even the tallest mid-latitude pedestals (<200 m) could form from deposits that accumulated in under 20 kyr.

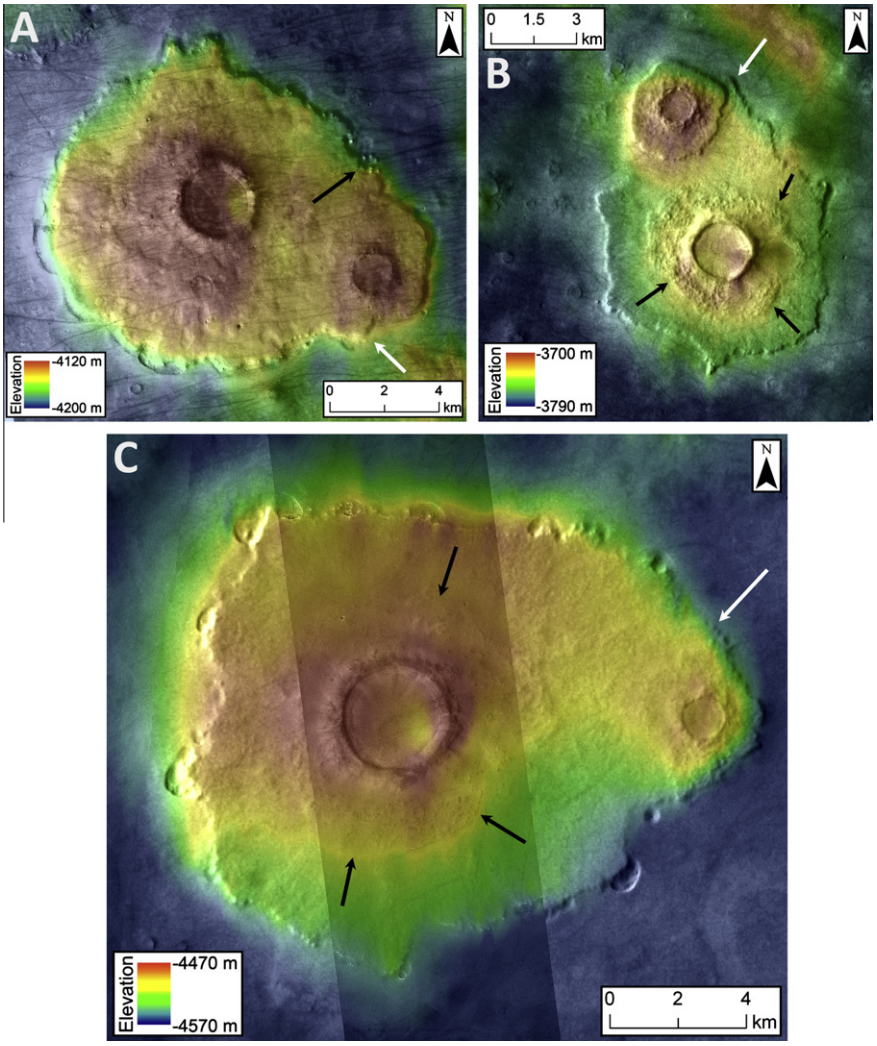

Fig. 7. Examples of pedestal craters that have marginal pits on their scarps and smaller pedestal craters draped or superposed on their margins. These cases show that superposed pedestal craters, which form from subsequent ice-rich deposits, are capable of partially preserving the radial extent of the underlying pedestal. The underlying pedestals gradually recede via the formation of sublimation pits, but are preserved due to subsequent armoring from the emplacement of the superposed pedestals. In all examples, the farthest extents of the underlying pedestals are directly adjacent to the superposed pedestals, as indicated by white arrows. (A) Pedestal craters (60.3°N, 188.6°E) shown in CTX image B02_010584_2407 with MOLA topography. The black arrow identifies possible mass wasting of the pedestal margin, where blocky material is contained in a shallow marginal pit. (B) Pedestal craters (57.1°N, 78.5°E) shown in THEMIS VIS image V21415004 with MOLA topography. Black arrows point to the distal rim of the ejecta deposit, which is clearly less extensive than the armored pedestal surface. (C) Pedestal craters (56.9°N, 106.9°E) shown in a THEMIS VIS (V13714004 and V28315004) and HiRISE (ESP_016600_2370) mosaic with MOLA topography. Black arrows identify the distal margin of the ejecta deposit superposed on the pedestal surface.

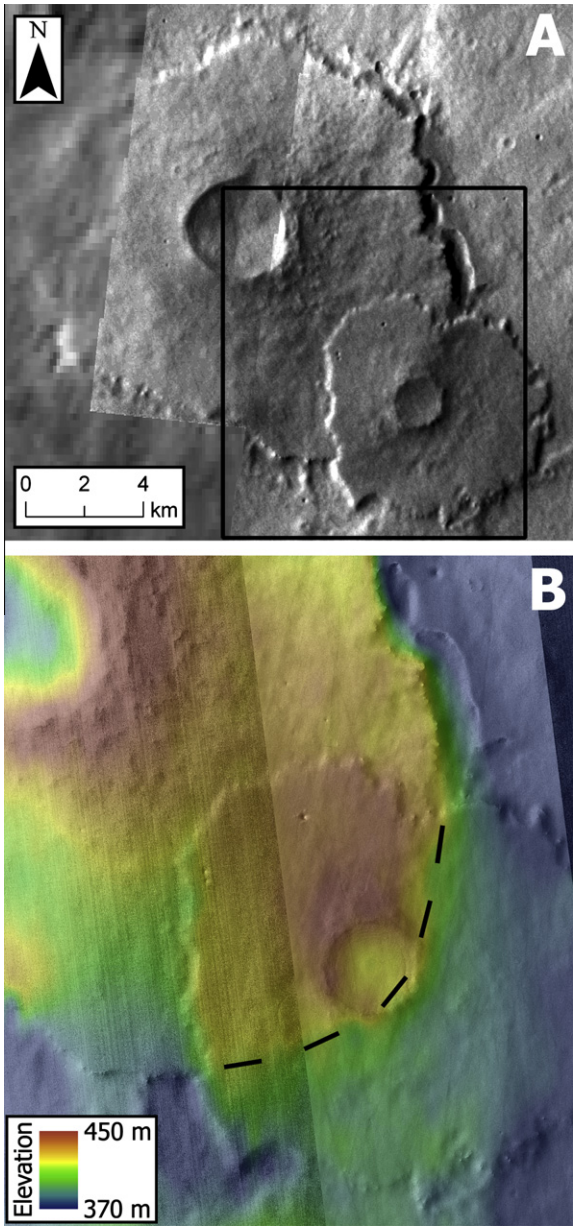

Fig. 8. An example of a draped pedestal crater. The smaller pedestal crater partially overlaps the larger pedestal crater, truncating the marginal pits in the larger pedestal's eastern scarp. (A) A mosaic of THEMIS VIS images V18046009 and V18358008 (61.0°S, 71.0°E). The black box delineates the area shown in part (B). Note that, on both craters, the ejecta deposits are faintly visible, and have radial extents that are less than half of their respective pedestals. (B) A mosaic of CTX image B08_012857_1187 and HiRISE image ESP_012857_1185, with MOLA topography. The MOLA data reveal the distinct topographic influence that the larger pedestal has on the smaller, draped pedestal; the buried scarp of the larger pedestal can be readily traced along the surface of the smaller pedestal, as shown by the black dashed line.

5.3. Pedestals with marginal pits

Some mid-latitude pedestal craters, concentrated in Utopia Planitia and Malea Planum, have pits along their marginal scarps (Figs. 7 and 8; also see Fig. 2 in Kadish et al. (2008)). As mentioned, these pits represent a loss of material from the pedestal itself; the pits occur in the scarps and do not excavate to depths lower than the surrounding terrain (Kadish et al., 2008). Contrary to recent research on morphologically similar pits in Utopia Planitia (Soare et al., 2008), we see no evidence for melting associated with these pits that would lead us to identify them as thermokarst lakes/alases.

The relatively even distribution of pits around pedestals – no preferred slope-facing orientation – provides important information about the sublimation process and the evolution of scarp formation and retreat. The even distribution indicates that asymmetric warming from insolation is not the primary factor responsible for where sublimation occurs. The slopes of pedestal margins are shallow, ranging from only 3° to 7°. For comparison, martian gullies, which exist predominantly on pole-facing slopes of crater walls, form on surfaces with an average slope of 26.5° (Dickson et al., 2007). The effect of uneven warming of pedestal scarp slopes is further diminished by the fact that pedestals with pits are located almost exclusively poleward of 50°N and 60°S, where the latitude-dependent temperature gradient is much less pronounced.

Although the sublimation rate of buried ice depends primarily on temperature (e.g. Mellon and Jakosky, 1993), it also is influenced by other factors, including atmospheric humidity, wind speed, till thickness, and surface albedo (e.g. Schorghofer and Aharonson, 2005; Kowalewski et al., 2006). As such, insolation is a contributing factor, but may not always be the dominant one. While the rate of diffusion of volatiles has important implications for the preservation of pedestal craters, it is not currently possible to constrain it quantitatively. Atmospheric conditions and regional temperatures have not been robustly established during the obliquity excursions necessary to produce pedestals. We also do not know the permeability of the armoring and how it varies as a function of distance from the crater rim. Future work using 1-D modeling and a better understanding of paleoclimatic conditions will help to assess these sublimation rates.

The presence of the pits guarantees that local meteorological conditions are conducive to sublimation, and insolation likely contributes to this. However, the radially symmetric distribution suggests that geologic factors play a more important role in establishing where the pits form. Specifically, the tapering or absence of the armoring along pedestal margins likely allows volatiles within the pedestal to diffuse into the atmosphere. In addition, the absence of pits on the pedestal surface supports the notion that the armoring is capable of significantly inhibiting sublimation of the underlying volatiles. If pits can form on both the equator- and pole-facing slopes of pedestal scarps, but not on the flat pedestal surfaces, which receive more insolation than the pole-facing scarps, then the thickness and/or degree of induration of the armoring must inhibit vapor diffusion, and thus drastically reduce the sublimation rate.

Although we do not frequently see evidence for significant mass wasting along pedestal margins, perhaps due to the shallowness of their slopes, it is likely that pit formation leads to scarp retreat, reducing the size of the pedestal (Figs. 7 and 10). Loss of volatiles from the edges of the pedestal results in downslope movement of material, which could degrade the integrity of the armoring along the perimeter of the pedestal. This would result in a positive feedback loop, allowing further pit formation, leading to continued scarp retreat. While it is difficult to assess the degree to which a pedestal's size has been reduced due to sublimation along the margins, we do see examples of pit coalescence, resulting in moat-like structures that represent a substantial loss of volume from the pedestal (Kadish et al., 2008). In addition, we have observed examples of highly degraded, non-circular pedestals that contain pits, providing evidence that repeated pit formation via sublimation is capable of completely removing pedestals (Fig. 10).

In cases where we see stratigraphic relationships between pedestals, the overlying pedestal often preserves the underlying pedestal at the point of overlap, truncating pits or preventing pit formation along that portion of the underlying pedestal's margin. While superposed pedestals are themselves subject to sublimation and erosion (Figs. 3B and 7C), the additional armoring they provide

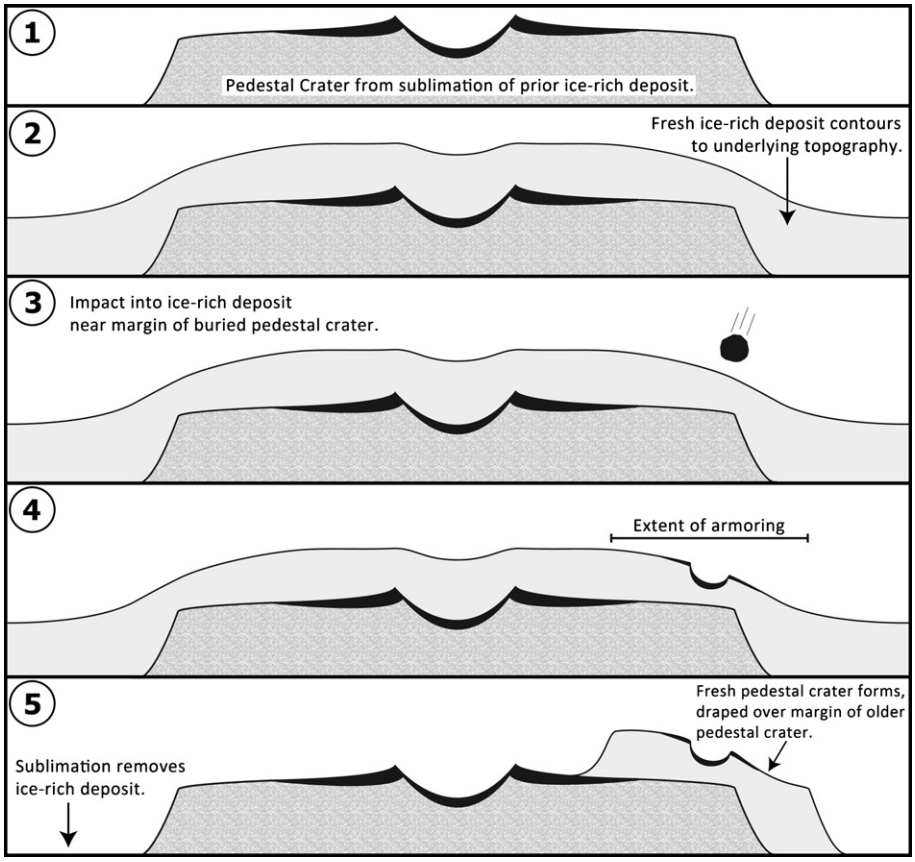

Fig. 9. A schematic diagram of the steps necessary to produce a pedestal crater draped over the marginal scarp of another pedestal crater, as seen in Fig. 8, where the smaller pedestal shows the topographic influence of the larger underlying pedestal. The steps are: (1) The presence of a pre-existing pedestal, which forms via the process shown in Fig. 1. (2) An obliquity excursion leads to the accumulation of a new ice-rich deposit that contours to the topography of the buried pedestal. (3) An impact occurs into this deposit at a point near the marginal scarp of the buried pedestal. This distributes ejecta and armors the proximal surface, as shown in steps 2 and 3 of Fig. 1. (4) The fresh crater bowl and armored surface are situated on the ice-rich deposit, stratigraphically above the margin of the underlying pedestal crater. (5) Return to a lower obliquity leads to sublimation of the regional ice-rich deposit, as shown in step 4 of Fig. 1. The armoring from the fresh crater, however, preserves some of the deposit, yielding a draped pedestal crater that contours to the topography of the underlying pedestal scarp.

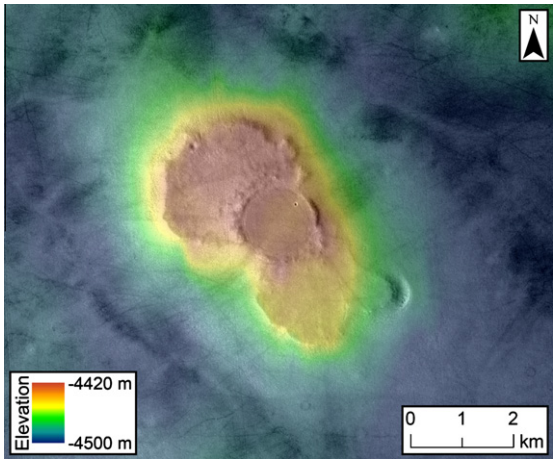

Fig. 10. The remnants of what was likely once a much larger pedestal crater, located at 58.2°N, 113.2°E. The CTX mosaic (P20_008754_2395 and P22_009822_2399) with MOLA topography shows that small portions of the pedestal remain preserved to the NW and SE of the infilled crater bowl. The pedestal is still perched more than 80 m above the surrounding terrain, and is surrounded by a halo of material that slopes gradually down to the plains. This supports the interpretation that pedestals sublimate and erode from their marginal scarps inward to their crater rims. In this instance, there is a marginal pit located on the SE portion of the pedestal scarp, and the pedestal surface is lower in elevation in that area.

is clearly effective in increasing the longevity of the underlying pedestal. This results in pedestal morphologies that appear to have been much larger, but have since sublimated and been eroded except where the overlying pedestals preserve their initial extents (Fig. 7).

The average height of pedestals with pits is 82.5 m, greatly exceeding the average height for the overall population. This indicates that having a greater scarp surface area is more conducive to sublimation from the margins of the pedestal, further supporting our interpretation that sublimation is limited by the geologic properties of the pedestal surface; if sublimation were controlled solely by insolation, then pedestals with pits should have the same average height as those without pits. The geographic restriction of these taller, pitted pedestals to Utopia Planitia and Malea Planum implies that these regions are unique in the timing and/or thicknesses of accumulation of the ice-rich deposits. Continued work in these geographic areas will explore whether these regions are more conducive to thicker deposits, which is consistent with the discussion in Section 5.1, or perhaps maintained deposits more recently than other regions and are thus still undergoing active sublimation.

6. Conclusions

On the basis of the sublimation-driven formation mechanism for pedestal craters, the current heights of the pedestals offer direct evidence for the approximate elevations of the icy paleosurfaces at

the times of impact. The pedestal heights act as a proxy for the thicknesses of the paleodeposits, perhaps modified somewhat by subsequent effects including compaction, erosion, mantling, and sublimation. We measured the heights of 2300 pedestals between 60°N and 65°S using MOLA data (Fig. 4). Through the analysis of these data, in conjunction with previously measured pedestal crater attributes (Kadish et al., 2009), we conclude that: (1) While pedestals can reach up to ~260 m in height, 82% are <60 m and only ~2% are >100 m (Fig. 5A). (2) The mean mid-latitude pedestal heights are 48.0 m in the northern hemisphere and 40.4 m in the southern hemisphere (Table 1). (3) Neither hemisphere shows any significant variation in average pedestal height as a function of latitude. However, taller pedestals (>80 m) tend to be restricted to latitudes poleward of 50°, whereas shorter pedestals (20–50 m) have high population density throughout the mid latitudes. Longitudinal variations in average pedestal height are present (Fig. 5B–D), with the tallest pedestals located in Utopia and Acidalia Planitia and Malea Planum. (4) Pedestal height has no statistically significant correlation with pedestal crater diameter, P/C ratio, or pedestal circularity (Fig. 6). This supports the interpretation that the final height of a pedestal is determined by the thickness of the ice-rich target deposit and not the impact process. (5) Pedestal craters with significantly different heights are found in close proximity to each other. Pedestals can also be partially draped or completely superposed on other pedestals (Figs. 7 and 8). This implies multiple distinct episodes of the deposition of a mid-latitude ice-rich layer. (6) Pedestal craters with marginal sublimation pits have a mean height of 82.5 m. These tall craters, which are located exclusively in Utopia Planitia and Malea Planum, indicate that these geographic regions may be more conducive to the accumulation of ice-rich material, or may have experienced more recent emplacement of an ice-rich deposit.

Acknowledgments

The authors are grateful for financial support from NASA Mars Data Analysis Program (MDAP) Grant NNX07AN95G and NASA Applied Information Systems Research Program NNX08AC63G to JWH, and MDAP Grant NAG512510 to NGB. SJK would like to thank Jay Dickson and Caleb Fassett for productive dialog on sublimation processes, as well as Joseph Boyce and an anonymous reviewer for constructive comments that strengthened this manuscript.

References

Arvidson, R.E., Coradini, M., Carusi, A., Coradini, A., Fulchignoni, M., Federico, C., Funiciello, R., Salomone, M., 1976. Latitudinal variation of wind erosion of crater ejecta deposits on Mars. Icarus 27, 503–516.

Barlow, N.G., 1994. Sinuosity of martian rampart ejecta deposits. J. Geophys. Res. 99, 10927–10935.

Barlow, N.G., 2004. Martian subsurface volatile concentrations as a function of time: Clues from layered ejecta craters. Geophys. Res. Lett. 31, L05703. doi:10.1029/2003GL019075.

Barlow, N.G., 2006. Impact craters in the northern hemisphere of Mars: Layered ejecta and central pit characteristics. Meteorit. Planet. Sci. 41 (10), 1425–1436.

Barlow, N.G., Boyce, J.M., Costard, F.M., Craddock, R.A., Garvin, J.B., Sakimoto, S.E.H., Kuzmin, R.O., Roddy, D.J., Soderblom, L.A., 2000. Standardizing the nomenclature of martian impact crater ejecta morphologies. J. Geophys. Res. 105, 26733–26738.

Barlow, N.G., Koroshetz, J., Dohm, J.M., 2001. Variations in the onset diameter for martian layered ejecta morphologies and their implications for subsurface volatile reservoirs. Geophys. Res. Lett. 28. doi:10.1029/2000GL012804.

Bleacher, J.E., Sakimoto, S.E.H., Garvin, J.B., Wong, M., 2003. Deflation/erosion rates for the Parva Member, Dorsa Argentea Formation and implications for the south polar region of Mars. J. Geophys. Res. 108. doi:10.1029/2001JE001535.

Boyce, J.M., Barlow, N.G., Tornabene, L.L., 2008. Lonar crater on Mars: Implications of its unusual morphology. Luanr Planet. Sci. XXXIX. Abstract 1406 (CD-ROM).

Dickson, J.L., Head, J.W., Kreslavsky, M., 2007. Martian gullies in the southern mid-latitudes of Mars: Evidence for climate-controlled formation of young fluvial features based upon local and global topography. Icarus 188, 315–323.

Forget, F., Haberle, R.M., Montmessin, F., Levrard, B., Head, J.W., 2006. Formation of glaciers on Mars by atmospheric precipitation at high obliquity. Science 311, 368–371.

Head, J.W., Mustard, J.F., Kreslavsky, M.A., Milliken, R.E., Marchant, D.R., 2003. Recent ice ages on Mars. Nature 426, 797–802.

Kadish, S.J., Head, J.W., Barlow, N.G., Marchant, D.R., 2008. Martian pedestal craters: Marginal sublimation pits implicate a climate-related formation mechanism. Geophys. Res. Lett. 35, L16104. doi:10.1029/2008GL034990.

Kadish, S.J., Barlow, N.G., Head, J.W., 2009. Latitude dependence of martian pedestal craters: Evidence for a sublimation-driven formation mechanism. J. Geophys. Res. 114, E10001. doi:10.1029/2008JE003318.

Kowalewski, D.E., Marchant, D.R., Levy, J.S., Head, J.W., 2006. Quantifying low rates of summertime sublimation for buried glacier ice in Beacon Valley, Antarctica. Antarct. Sci. 18 (3), 5–8. doi:10.1017/S0954102006000460.

Laskar, J., Correia, A.C.M., Gastineau, M., Joutel, F., Levrard, B., Robutel, P., 2004. Long term evolution and chaotic diffusion of the insolation quantities of Mars. Icarus 170 (2), 343–364.

Levrard, B., Forget, F., Montmessin, F., Laskar, J., 2004. Recent ice-rich deposits formed at high latitudes on Mars by sublimation of unstable equatorial ice during low obliquity. Nature 431, 1072–1075.

Madeleine, J.-B., Forget, F., Head, J.W., Levrard, B., Montmessin, F., Millour, E., 2009. Amazonian northern mid-latitude glaciation on Mars: A proposed climate scenario. Icarus 203, 390–405.

McCauley, J.F., 1973. Mariner 9 evidence for wind erosion in the equatorial and mid-latitude regions of Mars. J. Geophys. Res. 78, 4123–4137.

Mellon, M.T., Jakosky, B.M., 1993. Geographic variations in the thermal and diffusive stability of ground ice on Mars. J. Geophys. Res. 98, 3345–3364.

Mischna, M.A., Richardson, M.I., Wilson, R.J., McCleese, D.J., 2003. On the orbital forcing of martian water and CO_2 cycles: A general circulation model study with simplified volatile schemes. J. Geophys. Res. 108. doi:10.1029/2003JE002051.

Mouginis-Mark, P., 1979. Martian fluidized crater morphology – Variations with crater size, latitude, altitude, and target material. J. Geophys. Res. 84, 8011–8022.

Mutch, P., Woronow, A., 1980. Martian rampart and pedestal craters' ejecta-emplacement: Coprates quadrangle. Icarus 41 (2), 259–268.

Osinski, G.R., 2006. Effect of volatiles and target lithology on the generation and emplacement of impact crater fill and ejecta deposits on Mars. Meteorit. Planet. Sci. 41 (10), 1571–1586.

Richardson, M.I., Wilson, R.J., 2002. Investigation of the nature and stability of the martian seasonal water cycle with a general circulation model. J. Geophys. Res. 107. doi:10.1029/2001JE001536.

Schorghofer, N., Aharonson, O., 2005. Stability and exchange of subsurface ice on Mars. J. Geophys. Res. 110. doi:10.1029/2004JE002350.

Schultz, P.H., Lutz, A.B., 1988. Polar wandering of Mars. Icarus 73, 91–141.

Schultz, P.H., Mustard, J.F., 2004. Impact melts and glasses on Mars. J. Geophys. Res. 109. doi:10.1029/2002JE002025.

Soare, R.J., Osinski, G.R., Roehm, C.L., 2008. Thermokarst lakes and ponds on Mars in the very recent (Late Amazonian) past. Earth Planet. Sci. Lett. 272, 382–393.

Tanaka, K.L., Rodriguez, J.A.P., Skinner Jr., J.A., Bourke, M.C., Fortezzo, C.M., Herkenhoff, K.E., Kolb, E.J., Okubo, C.H., 2008. North polar region of Mars: Advances in stratigraphy, structure, and erosional modification. Icarus 196 (2), 318–358.

Thomson, B.J., Schultz, P.H., 2007. The geology of the Viking Lander 2 site revisited. Icarus 191 (2), 505–523.

Wrobel, K., Schultz, P., Crawford, D., 2006. An atmospheric blast/thermal model for the formation of high-latitude pedestal craters. Meteorit. Planet. Sci. 41 (10), 1539–1550.